

1 **Proteomic characterization of pilot scale hot-water extracts from the industrial carrageenan red**

2 **seaweed *Eucheuma denticulatum***

3

4 Simon Gregersen<sup>1\*</sup>, Margarita Pertseva<sup>2,3</sup>, Paolo Marcatili<sup>2</sup>, Susan Løvstad Holdt<sup>4</sup>, Charlotte Jacobsen<sup>4</sup>,

5 Pedro J. García-Moreno<sup>4,5</sup>, Egon Bech Hansen<sup>4</sup>, Michael Toft Overgaard<sup>1</sup>

6

7 <sup>1</sup> Department of Chemistry and Bioscience, Aalborg University, Denmark

8 <sup>2</sup> Department of Bio and Health Informatics, Technical University of Denmark, Denmark

9 <sup>3</sup> Department of Biosystems Science and Engineering, ETH Zurich, Switzerland

10 <sup>4</sup> National Food Institute, Technical University of Denmark, Denmark

11 <sup>5</sup> Department of Chemical Engineering, University of Granada, Spain

12

13 **Abstract:**

14 Seaweeds have a long history as a resource for polysaccharides/hydrocolloids extraction for use in the food

15 industry due to their functionality as stabilizing agents. In addition to the carbohydrate content, seaweeds

16 also contains a significant amount of protein, which may find application in food and feed. Here, we

17 present a novel combination of transcriptomics, proteomics, and bioinformatics to determine the protein

18 composition in two pilot-scale extracts from *Eucheuma denticulatum* (Spinosum) obtained via hot-water

19 extraction. The extracts were characterized by qualitative and quantitative proteomics using LC-MS/MS and

20 a *de-novo* transcriptome assembly for construction of a novel proteome. Using label-free, relative

21 quantification, we were able to identify the most abundant proteins in the extracts and determined that

22 the majority of quantified protein in the extracts (>75%) is constituted by merely three previously

\* Corresponding author: sgr@bio.aau.dk – Frederik Bajers Vej 7H – DK-9220 Aalborg – Denmark

23 uncharacterized proteins. Putative subcellular localization for the quantified proteins was determined by  
24 bioinformatic prediction, and by correlating with the expected copy number from the transcriptome  
25 analysis, we determined that the extracts were highly enriched in extracellular proteins. This implies that  
26 the method predominantly extracts extracellular proteins, and thus appear ineffective for cellular  
27 disruption and subsequent release of intracellular proteins. Ultimately, this study highlight the power of  
28 quantitative proteomics as a novel tool for characterization of alternative protein sources intended for use  
29 in foods. Additionally, the study showcases the potential of proteomics for evaluation of protein extraction  
30 methods and as powerful tool in the development of an efficient extraction process.

31

32 **Keywords**

33 *Eucheuma denticulatum*; hot-water protein extraction; quantitative proteomics; *de novo* quantitative  
34 transcriptomics; bioinformatics; subcellular localization

35

36 **1. Introduction:**

37 Seaweeds are known to contain numerous compounds of interest, such as polysaccharides, proteins and  
38 other compounds with health beneficial properties such as anti-inflammatory, anti-oxidant, and anti-cancer  
39 (Holdt & Kraan, 2011; Leandro et al., 2020). The industry to produce hydrocolloids from seaweed is well  
40 established, and the hydrocolloids are used as e.g. stabilizing agents in toothpaste, canned whipped cream,  
41 and as meat glue. The production of red carrageenan accounts for 54,000 ton/year and constitutes the  
42 majority of the total hydrocolloids sold worldwide (also incl. alginate and agar). Carrageenan is extracted  
43 from 212,000 ton dried seaweed, and brings in a value of 530 million USD (Porse, 2018). *Eucheuma*  
44 *denticulatum* is among the most cultivated and harvested red seaweed species for the carrageenan  
45 industry. However, at present carrageenan is extracted in a process, which extracts carrageenan as the only  
46 compound whereas proteins and other compounds are not extracted. The most common industrial method

47 to extract carrageenan from *Eucheuma denticulatum* uses hot water at high pH. If further extraction of  
48 other compounds such as proteins could be made prior to or as part of the industrial hot water extraction  
49 without compromising the existing carrageenan extraction, this could be of interest, since the amount of  
50 biomass available is large. Proteins from *E. denticulatum* were shown to constitute only 3.8% of dry  
51 biomass, but were of high quality with respect to their amino acid profile (Naseri, Jacobsen, et al., 2020).  
52 Moreover, the obtained proteins are comparable to beef in regard to the branched chained amino acids  
53 (i.e. leucine, isoleucine, and valine) that are of interest due to their muscle building properties.

54 In addition to the general health benefits from ingestion (Gomez-Zavaglia, Prieto Lage, Jimenez-Lopez,  
55 Mejuto, & Simal-Gandara, 2019; Peñalver et al., 2020), seaweed may also be a source of bioactive peptides  
56 that could exhibit a direct biological purpose or be utilized as functional food ingredients. These peptides  
57 can be released through bio-processing of proteins extracts using e.g. enzymatic hydrolysis or fermentation  
58 (Admassu, Gasmalla, Yang, & Zhao, 2018). In the past decade, peptides derived from seaweed proteins with  
59 e.g. renin-inhibitory (Fitzgerald et al., 2012), ACE-inhibitory (Furuta, Miyabe, Yasui, Kinoshita, & Kishimura,  
60 2016), antioxidant (Cian, Garzón, Ancona, Guerrero, & Drago, 2015), and antidiabetic (Harnedy &  
61 FitzGerald, 2013b) activities have been identified. Common for all bioactive peptides is that they were  
62 identified in enzymatic hydrolysates by a non-targeted trial-and-error approach. This methodology,  
63 commonly employed in the food industry, requires numerous costly and time-demanding steps of  
64 hydrolysis, separation, isolation, identification, and finally *in vitro* or *in vivo* verification of activity. In  
65 contrast, an orthogonal approach utilizing bioinformatic prediction of bioactive peptides, is gathering  
66 increased attention (Tu, Cheng, Lu, & Du, 2018). This method reduces cost and work load tremendously,  
67 and allows for targeted peptide release by enzymatic hydrolysis. With recent advances in bioinformatic  
68 prediction of peptide functionality (García-Moreno, Jacobsen, et al., 2020; Mooney, Haslam, Holton,  
69 Pollastri, & Shields, 2013; Mooney, Haslam, Pollastri, & Shields, 2012; Olsen et al., 2020; Panyayai et al.,  
70 2019), and the growing availability of peptide databases (Chen et al., 2013; Liu, Baggerman, Schoofs, &  
71 Wets, 2008; Minkiewicz, Iwaniak, & Darewicz, 2019; G. Wang, Li, & Wang, 2009), the primary prerequisite

72 for the analysis is the availability of protein sequences and quantitative information on protein  
73 composition. Recently, we employed quantitative proteomics for identification of abundant proteins  
74 followed by bioinformatic prediction (EmulsiPred source code freely available at  
75 <https://github.com/MarcatiliLab/EmulsiPred>) to identify a number of highly functional emulsifier peptides  
76 from potato (García-Moreno, Gregersen, et al., 2020) as well predicting probable emulsifier and antioxidant  
77 peptides in hydrolysates from fish processing side streams following LC-MS/MS analysis (Jafarpour, Gomes,  
78 et al., 2020; Jafarpour, Gregersen, et al., 2020). Nevertheless, proteomic quantification of the starting  
79 material is an absolute necessity in order to maximize the yield of peptide release. Here, we present a  
80 proteomic characterization of two industrially relevant, pilot-scale extracts from *E. denticulatum* obtained  
81 by hot-water extraction. Protein identification is based on a *de novo* transcriptome assembly for creating a  
82 novel reference proteome. Furthermore, we present a novel approach for quantifying proteins based on  
83 non-tryptic peptides, and correlate protein abundance with quantitative transcriptomics. Using  
84 bioinformatic prediction of protein subcellular origin, we are able to determine enrichment of certain  
85 protein classes in the extracts.

86

87 **2. Materials and Methods**

88 *2.1. Materials*

89 Two *Eucheuma denticulatum* protein extracts obtained using near-neutral, hot-water extraction were  
90 supplied by the global food ingredient provider CP Kelco. Protein extract A was obtained by dispersing the  
91 raw seaweed in deionized water (pH adjusted to 8.9 with sodium carbonate) and applying continuous  
92 stirring at 95°C for 5 h. The slurry was subsequently filtered in a Büchner funnel followed by diafiltration  
93 using a 300 kDa MWCO membrane. The retentate was washed with three volumes of 0.9% sodium chloride  
94 in deionized water, and all permeates were subsequently pooled. The pooled permeate was then  
95 concentrated using a 1 kDa MWCO membrane, and the retentate lyophilized to yield the final protein

96 extract A. Protein extract B was obtained similarly to extract A, but with stirring at 90°C for 16 h before  
97 filtering, diafiltration, concentration, and lyophilization. Furthermore, the lyophilized retentate was  
98 dissolved in deionized water, the pH was adjusted to 2.9 with nitric acid, and the mixture was stirred at  
99 room temperature for 1 h. Precipitated protein was isolated by centrifugation and washed twice with  
100 isopropanol before air drying and lyophilization to yield the final protein extract B. The total protein  
101 content of protein extracts A and B (by Kjeldahl-N) was 7.1% and 70% (w/w), respectively, using a nitrogen-  
102 to-protein conversion factor of 6.25 (CP Kelco supplied information). All chemicals used were of analytical  
103 grade.

104

105 *2.2. Total soluble protein*

106 Protein extracts A and B were solubilized to an estimated protein concentration of 2 mg/mL in ddH<sub>2</sub>O and  
107 in 200 mM NH<sub>4</sub>HCO<sub>3</sub> with 0.2% SDS for maximal solubilization compatible with the Qubit protein assay.  
108 Following solvent addition, samples were vortexed for 30 s, sonicated for 30 min, and left overnight on a  
109 Stuart SRT6 roller mixer (Cole-Parmer, UK). The next day, samples were sonicated for 30 min, left on a roller  
110 mixer for 60 min, and centrifuged at 3,095 RCF (ambient temperature) for 10 min in a 5810 R centrifuge  
111 (Eppendorf, Germany), prior to aliquoting the supernatant. The total soluble protein content of the samples  
112 in both solvents, was quantified using Qubit protein assay (Thermo Scientific, Germany) according to the  
113 manufacturer guidelines.

114

115 *2.3. 1D-SDS-PAGE and in-gel digestion.*

116 Protein extracts A and B were solubilized with 2% SDS in 200 mM ammonium bicarbonate (pH 9.5) to a final  
117 protein/peptide concentration of 2 mg/mL based on protein content by Kjeldahl-N. Alkaline buffer with  
118 detergent was used to maximize protein solubilization. Solubilization was further promoted by. Samples  
119 were vortexed for 2 min, sonicated for 30 min, and subsequently centrifuged at 3,095 RCF for 15 min to

120 precipitate solids. SDS-PAGE analysis was performed on precast 4-20% gradient gels (GenScript, USA) in a  
121 Tris-MOPS buffered system under reducing conditions according to manufacturer guidelines. Briefly, 20 µg  
122 protein/peptide was mixed with reducing (final DTT concentration 50 mM) SDS-PAGE sample buffer and  
123 subsequently denatured at 95 °C for 5 min prior to loading on the gel. As molecular weight marker, PIERCE  
124 Unstained Protein MW Marker P/N 26610 (ThermoFisher Scientific, USA) was used. Protein visualization  
125 was achieved by using Coomassie Brilliant Blue G250 staining (Sigma-Aldrich, Germany) and imaging with a  
126 ChemDoc MP Imaging System (Bio-Rad, USA).

127 Proteins were in-gel digested according to Shevchenko et al. (Shevchenko, Wilm, Vorm, & Mann, 1982) and  
128 Fernandez-Patron et al. (Fernandez-Patron et al., 1995), as previously described (García-Moreno,  
129 Gregersen, et al., 2020). Briefly, each gel lane from the gradient gel was excised with a scalpel and divided  
130 into 6 fractions guided by the MW marker (<14kDa; 14-25kDa; 25-45kDa; 45-66kDa; 66-116kDa; >116kDa).  
131 Individual fractions were cut into 1x1 mm pieces before being subjected to washing, reduction with DTT,  
132 Cys alkylation with iodoacetamide, and digestion with sequencing grade modified trypsin (Promega,  
133 Madison, WI, USA). Following digestion, peptides were extracted, dried down by SpeedVac, and suspended  
134 in 0.1% (v/v) formic acid (FA), 2% acetonitrile (ACN) (v/v). Next, peptides were desalted using StageTips  
135 (Fernandez-Patron et al., 1995; Rappaport, Mann, & Ishihama, 2007), dried down by SpeedVac, and finally  
136 suspended in 0.1% (v/v) FA, 2% ACN (v/v) for LC-MS/MS analysis.

137

138 *2.4. De novo transcriptome assembly.*

139 The transcriptome of *E. denticulatum* was downloaded from the NCBI SRA database  
140 (<https://www.ncbi.nlm.nih.gov/sra/SRX2653634>). The raw reads were preprocessed by Trimmomatic  
141 software to filter short sequences (less than 36 bp) and to trim low-quality ends (Bolger, Lohse, & Usadel,  
142 2014). Processed reads were then assembled *de novo* into contigs using Trinity with default parameters  
143 (Grabherr et al., 2011). Overall, 9458 contigs were assembled with an average length of 1021 bp.

144

145 *2.5. Transcript annotation, abundance estimation and protein database construction.*

146 The potential protein-coding sequences were predicted by TransDecoder based on the length of open  
147 reading frames and nucleotide composition (Grabherr et al., 2011). Candidate sequences were annotated  
148 by BlastP and BlastX search against SwissProt database (Madden, 2013) with the cutoff E-value of 1E-5 as  
149 well as by HMMER (Finn, Clements, & Eddy, 2011) search against Pfam database (El-Gebali et al., 2018; Finn  
150 et al., 2010). An alignment E-value of 1E-5 means that a homology hit has a 1 in 100,000 probability of  
151 occurring by chance alone, therefore we chose this threshold to get only high-quality homologous proteins  
152 hits.

153 The abundance of the transcripts (transcripts per megabase, TPM) was calculated by re-aligning reads to  
154 the assembled contigs using RSEM (RNA-Seq by Expectation-Maximization) estimation method included in  
155 Trinity software (Grabherr et al., 2011). Obtained transcript abundance matrix was joined with Blastp-  
156 annotated transcripts to attain a list of highly expressed proteins.

157

158 *2.6. Prediction of subcellular localization using deepLoc*

159 All proteins in the final database were analyzed by deepLoc (Almagro Armenteros, Sønderby, Sønderby,  
160 Nielsen, & Winther, 2017) using the freely available web-tool  
161 (<http://www.cbs.dtu.dk/services/DeepLoc/index.php>). All searches were performed using the BLOSUM62  
162 protein encoding to achieve a probability based subcellular localization for use in enrichment analysis on  
163 both transcriptome and protein level.

164

165        2.7. LC-MS/MS analysis

166        Tryptic peptides were analyzed by an automated LC-ESI-MS/MS consisting of an EASY-nLC system (Thermo  
167        Scientific, Bremen, Germany) on-line coupled to a Q Exactive mass spectrometer (Thermo Scientific) via a  
168        Nanospray Flex ion source (Thermo Scientific), as previously reported (García-Moreno, Gregersen, et al.,  
169        2020). Separation of peptides was achieved by use of an Acclaim Pepmap RSLC analytical column (C18, 100  
170        Å, 75 µm. x 50 cm (Thermo Scientific)). Instrumental settings, solvents, flows, gradient, and acquisition  
171        method were identical to what was described previously.

172

173        2.8. Proteomics data analysis

174        Protein identification and quantification was performed using MaxQuant 1.6.0.16. (Cox & Mann, 2008;  
175        Tyanova, Temu, Sinitcyn, et al., 2016) using the *de-novo* proteome assembled from the transcriptomic  
176        analysis. Initially, standard settings were employed using specific digestion (Trypsin/P, 2 missed cleavages  
177        allowed, minimum length 7 AAs) and false discovery rate (FDR) of 1% on both peptide and protein level.  
178        FDR was controlled using reverse decoy sequences and common contaminants were included. Protein  
179        quantification was obtained with including both unique and razor peptides. Samples were analyzed as six  
180        fractions with boosted identification rates by matching between runs and dependent peptides enabled. The  
181        iBAQ algorithm (Schwahnüsser et al., 2011) was used for relative in-sample protein quantification. iBAQ  
182        intensities were normalized to the sum of all iBAQ intensities after removal of reverse hits and  
183        contaminants, to obtain the relative iBAQ (riBAQ), as previously described (García-Moreno, Gregersen, et  
184        al., 2020; Shin et al., 2013).

185        MS-data were furthermore analyzed both semi-specifically (tryptic *N*- or *C*-terminus) and unspecifically (no  
186        terminal restrictions) in MaxQuant. All settings were maintained except for applying unspecific digestion  
187        with peptide length restrictions from 4 to 65 AAs. Additional unspecific searches with peptide and protein  
188        level FRD of 5% and 10% as well as semi-specific searches with peptide and protein level FRD of 5% was

189 conducted to increase identification rates and sequence coverage for comparison and data quality  
190 assessment.

191 Relative quantification with iBAQ employs strict tryptic restrictions to peptide termini and consequently,  
192 this type of quantifications is not possible for semi-specific and unspecific searches. In order to compare  
193 and evaluate the semi-specific and unspecific results, we introduced two additional quasi-quantitative  
194 relative metrics: i) relative intensity,  $I_{rel}$  and ii) length-normalized relative intensity,  $I^L_{rel}$ . They were defined  
195 as:

$$196 \quad I_{rel}(n) = \frac{I_n}{\sum_{n=1}^p I_n} * 100\% \quad (\text{Eq. 1})$$

$$197 \quad I^L_{rel}(n) = \frac{I_n/L_n}{\sum_{n=1}^p I_n/L_n} * 100\% \quad (\text{Eq. 2})$$

198 Where  $I_n$  is the intensity of protein n of p quantified proteins in a given sample and  $L_n$  is the length of  
199 protein n, based on the processed protein database. For evaluation of the two metrics, relative protein  
200 abundance was plotted as scatter plots between the different analysis conditions and the Pearson  
201 correlation coefficient (PCC) was calculated in Perseus (Tyanova, Temu, Sinitcyn, et al., 2016).

202 For final protein quantification, MS data were analyzed as both tryptic and semi-trypic digests using the  
203 following optimized search criteria: Peptides per protein  $\geq 2$  (razor and unique), protein FDR = 0.05,  
204 unmodified peptide score  $> 40$ , peptide FDR = 0.005. Match between runs and dependent peptides were  
205 both disabled. This was done to alleviate false positive identifications and increase quantitative validity.  
206 Increasing FDR to 5% for the tryptic analysis did not affect identification and quantification due to the  
207 applied score threshold.

208

209 *2.9. Comparative analysis of transcriptomic and proteomic data*

210 Comparative analysis was done on both the protein and subcellular levels. To estimate molar transcript  
211 abundance, we calculated the relative TPM (rTPM) for the individual proteins to the sum of TPMs for all  
212 1628 proteins in the database. Using the predicted subcellular localization, we then estimated the relative  
213 distribution of proteins based on the transcriptome using rTPM. Finally, we correlated the transcriptome-  
214 based protein distribution with the actual protein distribution for the extracts in a relative, quantitative  
215 manner.

216

217 *2.10. Data analysis and visualization*

218 Statistical and correlation analysis of transcriptome and MS data was performed in Perseus 1.6.1.3  
219 (Tyanova & Cox, 2018; Tyanova, Temu, Sinitcyn, et al., 2016). Venn diagrams were plotted with jvenn  
220 (Bardou, Mariette, Escudié, Djemiel, & Klopp, 2014). Additional data visualization was obtained using  
221 OriginPro 8.5.0 SR1 (OriginLab Corporation, Northampton, MA, USA) and figures assembled in their final  
222 form using INKSCAPE version 0.92.3 (<https://inkscape.org/>).

223

224 **3. Results and Discussion:**

225 *3.1. Transcriptome assembly, protein annotation, and subcellular localization*

226 The transcriptome of *Eucheuma denticulatum* was de novo assembled using publicly deposited  
227 transcriptome data at NCBI SRA database. The quality of the assembly was estimated by basic contig  
228 statistics and percentage of the remapped reads. Both metrics indicated a high quality of the assembly with  
229 an N50 value of 1891bp (Table A.1) and more than 90% of the reads mapped back to the contigs (Table  
230 A.2). Based on the transcriptomic information, an *E. denticulatum* protein database was constructed for  
231 subsequent mass-spectrometry (MS) analysis. First, the protein-coding sequences were predicted and

232 identified their by BlastX and BlastP search as well as their protein family by searching against Pfam  
233 database. Then the transcript expression level was calculated in terms of transcripts per kilo megabase  
234 (TPM) and removed proteins with TPM below 100, which resulted in 1628 proteins retained for the  
235 database. The TPM threshold was applied in order to filter out any potentially erroneous reads. Although  
236 this may in fact also filter some proteins with low copy numbers from the database, the primary objective  
237 was to identify highly expressed and extracted proteins, and consequently do not regard this to have  
238 substantial influence. A full list of protein accessions and their associated TPMs, rTPMs, Pfam functions,  
239 BlastX targets, and BlastP targets can be found in Table A.3 and in the linked Mendeley data repository. The  
240 *de-novo* protein database for *E. denticulatum* can be found in .fasta format in Table A.4 as well as in the  
241 Mendeley data repository.

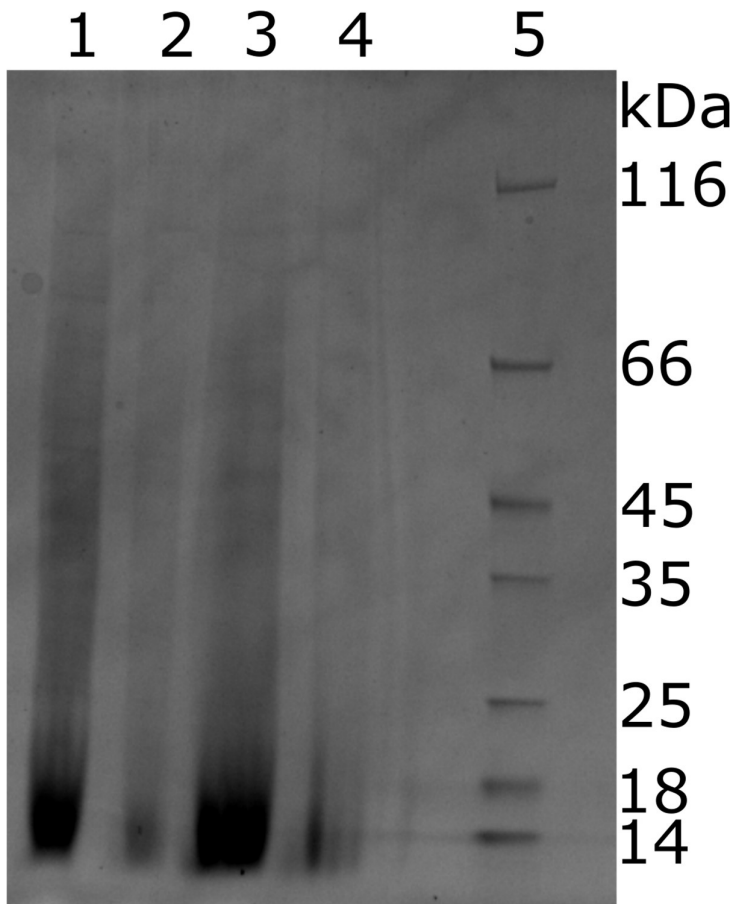
242 Although homology-inferred annotation using BLAST can indicate potential functions and localizations for  
243 the individual proteins, extraction of potential functions and subcellular localization on the proteome level  
244 is a tedious task. Additionally, as only verified Uniprot/Swiss-Prot proteins were included, the resulting  
245 annotations were of suboptimal quality (Table A.3) due to the lack of verified annotations on related and  
246 comparable species to *E. denticulatum*. Consequently, a bioinformatic prediction of subcellular localization  
247 on the individual protein level was used. This data type is easily binnable for large proteomes. As the  
248 DeepLoc neural network was developed for eukaryotic proteins with little or no available homology data  
249 (Almagro Armenteros et al., 2017), this directly applies to the case of this study. For the entire proteome,  
250 DeepLoc achieved a localization probability of  $0.63 \pm 0.21$  (Figure A.1).

251

### 252 3.2. 1D SDS-PAGE analysis and protein quality assessment

253 Both protein extracts display absence of distinct protein bands and an apparent smear along the gel  
254 concentrating in the low MW range, as seen from 1D SDS-PAGE analysis in Figure 1. This is in contrast to  
255 previous studies on *E. denticulatum* protein extracts (Rosni et al., 2015), where distinct protein bands were

256 observed and the low MW concentrated smear was absent. The significant difference in protein  
257 appearance by SDS-PAGE may be directly ascribed to the extraction method, as the authors here used a  
258 more elaborate protocol including organic (phenol) solvents as well as reducing conditions. Their approach  
259 may be significantly better for efficient extraction of intact proteins from the whole seaweed, but is not  
260 feasible on an industrial scale.



261

262 Figure 1: SDS-PAGE of *E. denticulatum* protein extracts investigated in this study. Protein loading is based  
263 on supplied protein content of 7.1% and 70% for extract A and B, respectively. 1: Extract A, 100 µg. 2:  
264 Extract A, 20 µg. 3: Extract B, 100 µg. 4: Extract B, 20 µg. 5: MW Marker.

265

266 The overall appearance of both extracts analyzed, however, are quite similar. The lack of distinct protein  
267 bands could potentially indicate partial hydrolysis during extraction using high temperature under alkaline  
268 conditions, as employed for both extraction methods. In addition, the extraction methodology employed  
269 may also result in co-extraction of other cellular moieties, which could interfere with electrophoresis and  
270 ultimately resulting in the observed smears. This has been reported for co-extracted lipids (Simões-  
271 Barbosa, Santana, & Teixeira, 2000; W. Wang et al., 2004), carbohydrates (Chart & Rowe, 1991; Hashimoto  
272 & Pickard, 1984), and DNA (Park, Kim, Choi, Grab, & Dumler, 2004). Further modification of proteins (e.g.  
273 glycoproteins) may also add to the smearing observed on SDS-PAGE (Elliott et al., 2004; Møller & Poulsen,  
274 2009; Sparbier, Koch, Kessler, Wenzel, & Kostrzewska, 2005).

275 In order to estimate the accuracy of the total protein by Kjeldahl-N analysis, we determined the soluble  
276 protein content in both aqueous solution and a slightly alkaline buffer with added detergent using Qubit  
277 protein assay (Table 1). From here, it is evident that the Kjeldahl-based total protein in fact correlates quite  
278 well with the soluble protein content – at least when solubilized in an alkaline buffer with detergent. A  
279 nitrogen-to-protein conversion factor of 6.25, the “Jones factor”, is commonly employed in food protein  
280 science and has been so for 90 years (Jones, 1931; Salo-Väänänen & Koivistoinen, 1996). Nevertheless, the  
281 universal conversion factor has been subject to several investigations, and species-dependent conversion  
282 factors are commonly recommended (Mariotti, Tomé, & Mirand, 2008). For seaweeds in particular, the  
283 factor can still vary significantly, but as no factor is available for *E. denticulatum*, a general conversion factor  
284 of 5.0 can be applied (Angell, Mata, de Nys, & Paul, 2016). By doing so, and thereby lowering the protein  
285 content by 20% (Table 1), the Kjeldahl-N method now underestimates the protein content compared to  
286 Qubit – in particular for extract B. In this respect, it is worth considering that the conversion factor is  
287 representative of the total organism proteome. Additionally, the non-protein nitrogen content of the  
288 extract is undetermined, and may also influence both the Kjeldahl-N and the Qubit outputs to some degree.

289 It is also evident that the aqueous solubility of the protein in the extracts is quite low (11-15% of the total  
290 protein), whereas a slightly alkaline buffer with a low amount of detergent practically fully solubilizes the  
291 protein (6-fold and 10-fold solubility increase for extract A and B, respectively). This also correlates well  
292 with the physical appearance of the solubilized extracts following centrifugation (Figure A.2), where a  
293 significantly higher amount of solid precipitate is visible in the aqueous solutions. Nevertheless, smear and  
294 apparent lack of intact high MW protein from SDS-PAGE must be taken into consideration for protein  
295 quantification and in the evaluation of the protein extracts as source for further processing as well as  
296 potential release of bioactive peptides.

297

Extract	Extraction method	Protein content (Kjeldahl-N * 6.25) <sup>1</sup>	Protein content (Kjeldahl-N * 5.0) <sup>2</sup>	Soluble protein (ddH <sub>2</sub> O)	Soluble protein (buffer)	Common contaminant proteins <sup>3</sup>	Verified Seaweed-specific proteins <sup>3</sup>
A	Alkaline, hot-water extraction → Ultracentrifugation → Lyophilization	7.1%	5.7%	1.1%	6.2%	20%	78%
B	Alkaline, hot-water extraction → Ultracentrifugation → Lyophilization → Acidic precipitation → Lyophilization	70%	56%	7.3%	74.8%	80%	6.0%

299 Table 1: General characteristics for the two *E. denticulatum* extracts analyzed in this work including total protein and soluble protein content. <sup>1</sup>Total  
 300 protein by Kjeldahl-N was supplied by CP Kelco. <sup>2</sup>Calculated based on supplied protein content (<sup>1</sup>) using a conversion factor of 5.0 (Angell et al., 2016).  
 301 <sup>3</sup>Sum of relative abundance for common contaminant proteins and verified seaweed specific proteins identified in MaxQuant by  $I_{rel}^L$  for semi-specific  
 302 analysis with optimized parameters, prior to any filtering, but after removing trypsin (Stage 1).

303        *3.3. Identification and quantification of peptides and proteins by LC-MS/MS*

304        Initially, we applied an iterative process where different *in silico* digestion methods (i.e. specific, semi-  
305        specific, and unspecific digestion), peptide- and protein-level FDR, and number of identified peptides per  
306        protein were attempted. This was done not only to identify the optimal parameters for analysis, but also to  
307        investigate the feasibility of applying the two specified quantitative metrics. The iterative process was of  
308        utmost importance, as the sample quality and especially the number of identified peptides and proteins for  
309        the extracts was low. A low number of peptide identifications significantly affects protein identification and  
310        quantification via the impact on FDR-controlled thresholds. This is ultimately an inherent property of the  
311        peptide scoring algorithm. MaxQuant employs the Andromeda search engine, in which peptide score is not  
312        only based on PEP, but also on the intensity of a given feature (Cox et al., 2011; Tiwary et al., 2019;  
313        Tyanova, Temu, & Cox, 2016). Consequently, high intensity features with significant PEP (i.e. potential false  
314        positives), which in other studies may have been filtered out, will obtain a sufficiently high peptide score  
315        and be used in protein quantification. Ultimately, this leads to false identification of proteins with a  
316        significant relative abundance, which impairs further analysis. By applying more stringent thresholds on  
317        both peptide and protein level, this is alleviated to some extent. Nevertheless, it may be needed to inspect  
318        and evaluate PEPs rather than apply threshold filtering on peptide score alone, as PEP relies solely on PSM  
319        and sequence-dependent features. This aspect is thoroughly discussed and evaluated in Appendix A.

320        By applying the optimized search parameters, a total of 66 proteins across both extracts and analysis  
321        methods (tryptic and semi-specific) following filtering of trypsin and reverse hits (Stage 1) were identified  
322        and quantified (Table 2). Extract B is highly contaminated since 80% (based on  $I_{\text{rel}}^L$  for semi-tryptic analysis)  
323        of all identified proteins were constituted by common contaminants (Table 1), primarily keratins. On the  
324        other hand, extract A “only” contained 20%. Although common contaminants are usually filtered out prior  
325        to quantification, the magnitude is noteworthy. In total, merely 40 proteins were identified across both  
326        extracts and analysis conditions, following filtering of common contaminants and subsequent re-  
327        quantification (Stage 2, Tables A.5; A.6). Semi-specific analysis resulted in identification of four additional

\* Corresponding author: sgr@bio.aau.dk – Frederik Bajers Vej 7H – DK-9220 Aalborg – Denmark

328 proteins (one in extract A and three in extract B), whereof one (c1275\_g1\_i1.p1) constitutes more than half  
329 of the Stage 2 protein by  $I^L_{rel}$  in extract B. Furthermore, 11 proteins were not identified by this approach  
330 (four in extract A, three in extract B and four identified in both extracts using tryptic conditions), but none  
331 of these were of high abundance. From plotting relative abundance by both riBAQ and  $I^L_{rel}$  (Figure A.3), a  
332 correlation was seen within each extract (PPC = 0.99-1.0 for extract A; PPC = 0.19-0.95 for extract B), but  
333 the semi-specific analysis of extract B correlated poorly with the tryptic analysis. The correlation between  
334 extracts was even worse (PPC = 0.14-0.55), indicating that the stringent quality parameters applied for  
335 automatic filtering, were not fully capable of cleaning the data from bad peptide spectrum matches (PSMs)  
336 and dubious protein identifications.

337

338

Stage 1								Stage 2								Stage 3							
Protein IDs	I <sup>L</sup> <sub>rel</sub> A tryp	riBAQ A	I <sup>L</sup> <sub>rel</sub> A semi	I <sup>L</sup> <sub>rel</sub> B tryp	riBAQ B	I <sup>L</sup> <sub>rel</sub> B semi	Contaminant ID	Protein IDs	I <sup>L</sup> <sub>rel</sub> A tryp	riBAQ A	I <sup>L</sup> <sub>rel</sub> A semi	I <sup>L</sup> <sub>rel</sub> B tryp	riBAQ B	I <sup>L</sup> <sub>rel</sub> B semi	Protein IDs	I <sup>L</sup> <sub>rel</sub> A tryp	riBAQ A	I <sup>L</sup> <sub>rel</sub> A semi	I <sup>L</sup> <sub>rel</sub> B tryp	riBAQ B	I <sup>L</sup> <sub>rel</sub> B semi		
CON__ENSEMBL	NQ	NQ	NQ	0.1%	0.1%	NQ	Keratin	rf1c10492_g1_i1.p1	NQ	NQ	NQ	0.1%	0.1%	NQ	rf1c1505_g2_i1.p1	8.6%	11.8%	13.4%	1.2%	1.5%	1.7%		
CON__O43790	NQ	NQ	NQ	0.7%	0.5%	0.6%	Keratin	rf1c1275_g1_i1.p1	NQ	NQ	NQ	NQ	NQ	11.1%	rf1c1613_g1_i1.p1	NQ	NQ	0.0%	0.0%	0.0%	0.0%		
CON__P02533	0.1%	0.1%	0.0%	1.9%	1.5%	1.8%	Keratin	rf1c1294_g1_i1.p1	0.0%	0.0%	NQ	0.0%	0.0%	NQ	rf1c17304_g1_i1.p1	2.6%	2.3%	2.5%	0.3%	0.2%	0.2%		
CON__P02662	NQ	NQ	NQ	0.1%	0.1%	NQ	α-S1-casein	rf1c1357_g1_i1.p1	NQ	NQ	NQ	0.0%	0.0%	NQ	rf1c17615_g1_i1.p1	0.1%	0.1%	NQ	NQ	NQ	NQ		
CON__P02666	0.0%	0.0%	0.0%	2.2%	3.8%	1.8%	β-casein	rf1c17161_g1_i1.p1	NQ	NQ	NQ	0.1%	0.0%	NQ	rf1c231_g1_i1.p1	0.1%	0.1%	NQ	NQ	NQ	NQ		
CON__P02754	6.5%	4.7%	6.9%	5.2%	3.7%	4.9%	β-lactoglobulin	rf1c17201_g1_i1.p1	0.0%	0.0%	NQ	NQ	NQ	NQ	rf1c2364_g1_i1.p1	0.1%	0.1%	0.1%	0.5%	0.4%	0.4%		
CON__P02768	0.0%	0.0%	0.0%	0.0%	0.0%	0.0%	Albumin	rf1c17231_g1_i1.p1	0.0%	0.0%	0.0%	0.3%	0.3%	0.2%	rf1c2556_g1_i1.p1	0.0%	0.0%	NQ	0.0%	0.0%	NQ		
CON__P02769	0.0%	0.0%	0.0%	1.5%	1.1%	1.3%	Albumin	rf1c2788_g1_i1.p1	NQ	NQ	NQ	NQ	NQ	0.2%	rf1c3760_g1_i1.p1	NQ	NQ	0.7%	NQ	NQ	NQ		
CON__P04264	5.5%	5.6%	4.6%	33.3%	33.1%	26.7%	Keratin	rf1c3249_g1_i1.p1	0.0%	0.0%	NQ	NQ	NQ	NQ	rf1c4090_g1_i1.p1	0.1%	0.1%	0.1%	0.0%	0.0%	NQ		
CON__P08779	0.0%	0.0%	0.0%	0.3%	0.2%	0.2%	Keratin	rf1c4757_g1_i1.p1	NQ	NQ	NQ	0.1%	0.1%	0.2%	rf1c4354_g1_i1.p1	3.3%	4.1%	3.1%	0.0%	0.0%	0.0%		
CON__P13645	6.2%	6.9%	5.5%	19.3%	21.1%	16.8%	Keratin	rf1c4921_g1_i1.p1	NQ	NQ	NQ	0.0%	0.0%	0.1%	rf1c4671_g1_i1.p2	0.3%	0.4%	0.2%	NQ	NQ	NQ		
CON__P13647	0.2%	0.2%	0.2%	1.8%	1.6%	0.9%	Keratin	rf1c5168_g1_i1.p1	NQ	NQ	NQ	0.0%	0.0%	0.1%	rf1c5232_g1_i1.p1	0.9%	0.9%	0.8%	NQ	NQ	NQ		
CON__P19013	NQ	NQ	0.0%	0.2%	0.1%	0.1%	Keratin	rf1c5952_g1_i1.p1	NQ	NQ	NQ	NQ	NQ	0.1%	rf1c6313_g1_i1.p1	27.2%	25.3%	25.2%	0.2%	0.2%	1.4%		
CON__P35527	1.1%	1.3%	1.1%	17.2%	19.7%	16.2%	Keratin	rf1c6797_g1_i1.p1	NQ	NQ	NQ	0.0%	0.0%	0.0%	rf1c6373_g1_i1.p1	0.0%	0.0%	0.0%	0.0%	0.0%	NQ		
CON__P35908	2.3%	1.8%	1.9%	6.1%	4.7%	5.9%	Keratin	rf1c6825_g1_i1.p3	1.4%	0.9%	1.3%	2.8%	1.7%	2.1%	rf1c6458_g1_i1.p1	1.1%	1.8%	1.4%	NQ	NQ	NQ		
CON__P48668	0.0%	0.0%	0.0%	0.6%	0.6%	1.3%	Keratin	rf1c6945_g1_i1.p2	0.0%	0.0%	0.0%	0.2%	0.2%	0.2%	rf1c6656_g1_i1.p1	0.0%	0.0%	0.0%	0.3%	0.3%	0.3%		
CON__P78386	0.0%	0.0%	NQ	0.1%	0.1%	0.1%	Keratin	rf1c8389_g1_i1.p1	0.0%	0.0%	NQ	0.1%	0.0%	NQ	rf1c6834_g1_i1.p3	0.0%	0.0%	NQ	0.0%	0.0%	NQ		
CON__Q04695	NQ	NQ	0.0%	0.2%	0.1%	0.2%	Keratin								rf1c6963_g2_i1.p1	0.1%	0.1%	0.0%	0.0%	0.0%	0.0%		
CON__Q14525	0.0%	0.0%	0.0%	0.1%	0.0%	0.0%	Keratin								rf1c7052_g1_i1.p1	27.0%	25.1%	25.8%	1.6%	1.5%	1.5%		
CON__Q5D862	0.0%	0.0%	NQ	0.0%	0.0%	NQ	Filaggrin-2								rf1c7052_g1_i2.p1	3.5%	3.9%	3.2%	0.4%	0.4%	0.4%		
CON__Q6KB66	NQ	NQ	NQ	0.0%	0.0%	NQ	Keratin								rf1c7216_g1_i1.p1	0.3%	0.3%	0.4%	NQ	NQ	NQ		
CON__Q9UE12	0.0%	0.0%	NQ	0.6%	0.5%	0.5%	Keratin								rf1c8421_g1_i1.p1	1.2%	2.0%	1.2%	NQ	NQ	NQ		
CON__Q9NSB2	NQ	NQ	NQ	0.1%	0.0%	0.0%	Keratin								rf1c926_g1_i1.p1	0.0%	0.0%	0.0%	NQ	NQ	NQ		
CON__Q7Z3Y8	NQ	NQ	NQ	0.0%	0.0%	0.0%	Keratin																
CON__Q86YZ3	NQ	NQ	NQ	0.0%	0.0%	0.0%	Hornerin																
CON__Q8IUT8	NQ	NQ	NQ	NQ	NQ	NQ	Keratin																

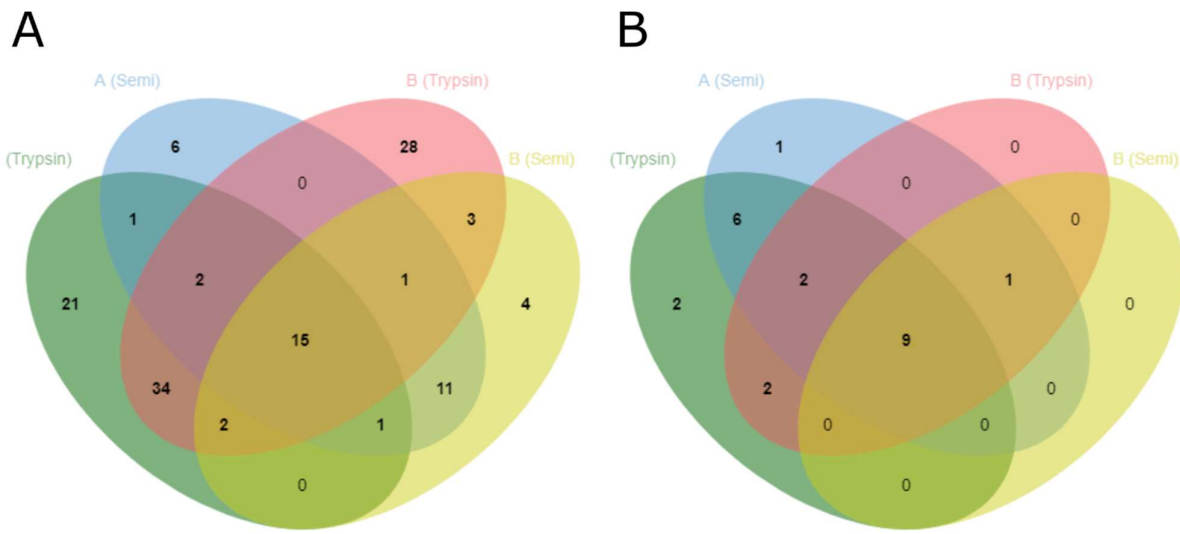
340 Table 2: Relative protein abundance of *E. denticulatum* extracts A and B (after filtering of trypsin) following  
341 initial quantification (Stage 1) with optimized search parameters by  $I^L_{\text{rel}}$  and riBAQ for both tryptic and semi-  
342 specific analysis. Proteins are divided in common contaminants (Stage 1 filtered proteins), false positive  
343 identifications/contaminants (Stage 2 filtered protein), and final, verified proteins (Stage 3). Common  
344 contaminants are annotated using their UniProt accession number. NQ: Protein not quantified in the  
345 specific sample using the specific analysis method.

346

347 Identified “outliers” (Tables A.5; A.6) that did not correlate between extracts (i.e. are suddenly highly  
348 enriched in extract B) may in fact be contaminants with some homology to the *E. denticulatum* proteome  
349 (further details are presented in the Appendix A). For instance, in the tryptic analysis of extract B,  
350 c6825\_g1\_i1.p3 is highly abundant but only identified by two peptides, which both map to histones from  
351 e.g. humans. Histone was also the BLASTX target (*Xenopus laevis* (African clawed frog) histone H2AX) as  
352 well as the predicted function by Pfam (Table A.3). Consequently, and because it was very low abundance  
353 in extract A, this was ascribed as contaminant to the extract and not originating from the seaweed.  
354 Although histones were bound to be identified in *E. denticulatum*, homologues from other organisms  
355 would bias quantification and it was consequently excluded. Furthermore, the highly abundant protein  
356 identified by semi-specific analysis of extract B only (c1275\_g1\_i1.p1), was also identified by only two  
357 peptides. As the protein score of 11.8 was very low (see Appendix A and Table A.6), and the posterior error  
358 probability (PEP) was significant (PEP>0.05), these were regarded bad PSMs and the protein ID was deemed  
359 false positive. Based on these observations, manual inspection and validation was performed in order to  
360 apply a final filtering step using the rationale described above. In the filtering, significant weight was put on  
361 evaluation of PEP rather than peptide score, as low scoring peptides (< 40) were pre-filtered in the  
362 optimized search parameters (see Appendix A for further details). Filtered proteins, along with the rationale  
363 for their exclusion, can be found in Table A.7 and proteins are listed under Stage 2 in Table 2.

364 Following filtering, verified proteins were re-quantified (Stage 3) the list of identified proteins was reduced  
365 from 40 to 23 proteins across extracts and conditions (Table 3). The stringent parameters applied in data  
366 analysis, as well requirements for inclusion in the final list, fully alleviated the problem of new and  
367 significantly abundant proteins showing up in extract B (see Table 2 and Figure A.3), as no proteins  
368 exclusive for extract B, were observed (Figure 2B). Nine proteins were observed exclusively in extract A, but  
369 this may be explained as loss during the extended processing for extract B. Extended processing may also  
370 be a likely explanation for the extract B exclusive peptides identified (Figure 2A). Furthermore, all nine  
371 proteins are of somewhat low abundance ( $I^L_{rel} < 2\%$ ), and do not affect the overall protein distribution  
372 significantly. Interestingly, the 9 proteins identified in both extracts using both analyses approaches,  
373 constituted > 93% of the verified protein in extract A and > 99% of the verified protein in extract B (by  $I^L_{rel}$ ).  
374 In fact, three proteins (c6313\_g1\_i1.p1, c7052\_g1\_i1.p1, and c1505\_g2\_i1.p1) constitute more than 75% of  
375 the total protein identified in both extracts (Table 3). Furthermore, an isoform of c7052\_g1\_i1  
376 (c7052\_g1\_i2), which only differs in the C-terminal region of the protein, was also identified in significant  
377 abundance. If included, the proteins constitute > 80% of the verified seaweed-specific protein in both  
378 extracts. With MW in the range 16-24 kDa, all three (four) proteins correlated well with the observations  
379 from SDS-PAGE (Figure 1), even though no clear protein bands were observed. This indicated that these  
380 three (four) proteins in particular may be of certain interest as potential sources of e.g. bioactive peptides.  
381 Protein sequences and experimental sequence coverage for the three major proteins are shown in Figure 3.  
382 From BlastP against verified proteins in UniProtKB/Swiss-Prot (Table S3), c7052\_g1\_i1.p1 (as well as the  
383 isoform) shows some homology to an immunogenic protein from *Brucella suis* (UniProt AC# P0A3U9),  
384 whereas Pfam indicates it could be related to the DNA repair protein REV1. Neither c6313\_g1\_i1.p1 nor  
385 c1505\_g2\_i1.p1 matched any proteins from the Blast homology or Pfam protein families. Consequently, the  
386 nature, structure, and function of the three highly abundant proteins remains unknown.  
387

388



389

390 Figure 2: 4-way Venn diagrams showing identified peptides (A) and proteins (B) with optimized parameters  
391 (5% FDR and minimum score threshold) and following filtering for extract A using tryptic analysis (green),  
392 extract A using semi-trypic analysis (blue), extract B using tryptic analysis (red), and extract B using semi-  
393 tryptic analysis (yellow). List sizes (in the same order) for peptides (A) are 76, 37, 85, and 37 for a total of  
394 129 identified peptides. List sizes (in the same order) for proteins (B) are 21, 19, 14, and 10 for a total of 23  
395 identified proteins.

396

397

Protein ID	MW [kDa]	#Pep		#Pep		#Pep		Seq. cov. A	Seq. cov. B	Seq. cov. A	Seq. cov. B	Score tryp	Score semi	riBAQ A tryp	I <sup>L</sup> <sub>rel</sub> A semi	I <sup>L</sup> <sub>rel</sub> A tryp	riBAQ B tryp	I <sup>L</sup> <sub>rel</sub> B tryp	I <sup>L</sup> <sub>rel</sub> B semi	rTPM	Subcellular localization <sup>1</sup>	Subcell score <sup>1</sup>
		A tryp	B tryp	A semi	B semi	tryp [%]	tryp [%]	tryp [%]	tryp [%]	tryp [%]	tryp [%]	tryp	tryp	tryp	tryp	tryp	tryp	tryp	tryp	tryp	tryp	
c6313_g1_i1.p1	21.153	7	1	13	5	36.3	7.4	47.9	17.4	323.3	323.3	32.3%	35.5%	<b>32.1%</b>	3.4%	3.8%	<b>23.3%</b>	0.29%	Extracellular	0.6985		
c7052_g1_i1.p1	24.213	7	8	16	7	36.1	34.8	45.4	31.7	323.3	323.3	31.9%	35.2%	<b>33.0%</b>	31.9%	35.9%	<b>25.1%</b>	0.02%	Extracellular	0.9128		
c1505_g2_i1.p1	15.778	4	4	7	5	30	30	30	30	323.3	323.3	15.1%	11.3%	<b>17.1%</b>	33.4%	25.4%	<b>28.0%</b>	0.14%	Extracellular	0.4441		
c4354_g1_i1.p1	40.332	8	1	7	3	24.6	3.5	21.7	5.6	323.3	323.3	5.2%	4.3%	<b>4.0%</b>	0.2%	0.1%	<b>0.3%</b>	0.15%	Extracellular	0.8483		
c7052_g1_i2.p1	23.965	6	5	15	5	30.8	25.1	40.1	25.1	163.3	140.2	4.9%	4.5%	<b>4.1%</b>	8.3%	7.8%	<b>6.8%</b>	0.06%	Extracellular	0.9431		
c17304_g1_i1.p1	27.965	6	2	6	1	23	6.7	19.7	3	188.3	190.4	2.9%	3.4%	<b>3.2%</b>	4.8%	5.7%	<b>3.5%</b>	1.08%	Extracellular	0.5089		
c8421_g1_i1.p1	59.681	4	0	4	1	10	0	10	2.3	323.3	323.3	2.6%	1.6%	<b>1.6%</b>	0.0%	0.0%	<b>0.0%</b>	0.04%	Membrane	0.9998		
c6458_g1_i1.p1	46.381	3	0	7	0	10.8	0	17.5	0	303.3	145.4	2.2%	1.4%	<b>1.8%</b>	0.0%	0.0%	<b>0.0%</b>	0.12%	Extracellular	0.8601		
c5232_g1_i1.p1	18.952	2	0	2	0	13.5	0	13.5	0	125.3	104.9	1.2%	1.1%	<b>1.1%</b>	0.0%	0.0%	<b>0.0%</b>	0.03%	Extracellular	0.6419		
c4671_g1_i1.p2	29.874	4	0	3	0	19.9	0	17	0	52.5	31.4	0.5%	0.4%	<b>0.2%</b>	0.0%	0.0%	<b>0.0%</b>	0.03%	Plastid	0.995		
c7216_g1_i1.p1	25.446	2	0	3	0	10.8	0	16.9	0	16.1	19.3	0.4%	0.3%	<b>0.4%</b>	0.0%	0.0%	<b>0.0%</b>	0.08%	Extracellular	0.8121		
c17615_g1_i1.p1	27.973	2	0	0	0	7.7	0	0	0	13.9	0.0	0.2%	0.2%	<b>0.0%</b>	0.0%	0.0%	<b>0.0%</b>	0.06%	Extracellular	0.9751		
c6963_g2_i1.p1	165.47	10	2	4	2	6.5	1.6	2.1	1.6	108.7	55.5	0.1%	0.1%	<b>0.1%</b>	0.5%	0.5%	<b>0.6%</b>	0.04%	Plastid	0.6933		
c4090_g1_i1.p1	16.129	1	2	1	1	6.8	12.9	6.8	6.1	15.3	11.2	0.1%	0.1%	<b>0.1%</b>	0.5%	0.7%	<b>0.0%</b>	0.02%	Plastid	0.9815		
c231_g1_i1.p1	18.006	2	0	0	0	10.2	0	0	0	11.7	0.0	0.1%	0.1%	<b>0.0%</b>	0.0%	0.0%	<b>0.0%</b>	0.05%	Extracellular	0.9998		
c2364_g1_i1.p1	50.492	1	5	2	5	2.4	9.9	4.1	9.9	135.4	105.1	0.1%	0.1%	<b>0.1%</b>	8.4%	10.8%	<b>6.9%</b>	0.23%	Cytoplasm	0.7655		
c926_g1_i1.p1	79.764	3	0	2	0	3.6	0	2.6	0	20.2	10.9	0.1%	0.1%	<b>0.1%</b>	0.0%	0.0%	<b>0.0%</b>	0.04%	Extracellular	0.9924		
c6373_g1_i1.p1	119.64	4	1	2	0	4.1	0.9	2.3	0	79.2	40.8	0.1%	0.0%	<b>0.0%</b>	0.1%	0.1%	<b>0.0%</b>	0.06%	Extracellular	0.5704		
c6656_g1_i1.p1	43.007	3	3	1	3	8.8	8.5	3.3	8.5	79.4	75.8	0.0%	0.0%	<b>0.0%</b>	7.0%	7.4%	<b>5.4%</b>	0.12%	Plastid	0.9982		
c6834_g1_i1.p3	22.388	1	1	0	0	5.3	6.7	0	0	15.3	0.0	0.0%	0.0%	<b>0.0%</b>	0.5%	0.7%	<b>0.0%</b>	0.06%	Plastid	0.9985		
c2556_g1_i1.p1	57.477	1	3	0	0	2	4.9	0	0	19.4	0.0	0.0%	0.0%	<b>0.0%</b>	0.8%	0.8%	<b>0.0%</b>	0.05%	Plastid	0.567		
c1613_g1_i1.p1	32.099	0	2	1	2	0	7.8	5.4	9.5	35.0	31.5	0.0%	0.0%	<b>0.0%</b>	0.4%	0.4%	<b>0.2%</b>	0.09%	Plastid	0.9671		
c3760_g1_i1.p1	32.533	0	0	3	0	0	0	6.6	0	0.0	253.1	0.0%	0.0%	<b>0.0%</b>	0.0%	1.0%	<b>0.0%</b>	0.06%	Lysosome	0.3775		

400 Table 3: Summary of verified proteins following parameter optimization, manual inspection, and filtering  
401 (Stage 3) for *E. denticulatum* extracts A and B using both tryptic and semi-trypic analysis. For each  
402 identified protein, the molecular weight, number of identified peptides, sequence coverage, protein score,  
403 riBAQ,  $I^L_{rel}$ , rTPM, subcellular localization, and localization probability. <sup>1</sup>Subcellular localization and  
404 localization probability was computed using DeepLoc (Almagro Armenteros et al., 2017).

405

```
>c1505_g2_i1.p1      TotalSequenceCoverage=30%
MSHKLLPSLLLLSFLLLLNFPPSTSSTPALSPPHKNPNNALSPHLQSITEEDDDDLTA
PSTLRRVFATPRVFNIIVRYRRFAPLALNADPETTSQIRAVLVVCLQQVRELQRDDNVRN
VRILLSSLVLLLDWLVCLLN*
```

```
>c6313_g1_i1.p1      TotalSequenceCoverage=52%
MALIWLISIVFALLTALGTTSAVNLPVLRVNANCNRDFPVRNNIRLRVRYVWNDMQTD
LDTSTRFLGENVGFACSGSAQTYLSFEGDNTGRGEEEVAIVEVGDKDEAWRGTTCIVL
KAQWFNSRNQGNIRVIVEIRNKGTNNLIRDPLEIVARPGVGDSCSMRLIATVVVDEDEGI
YLARAFNCPN*
```

```
>c7052_g1_i1.p1      TotalSequenceCoverage=54%
MTPLLLPLLLALTANTPHPTPRSISVTGDASVAAEPDIATLTTEVVTIAPTAQAALTR
NNRLTSALFDTLSEFNVSRRDIQTTFSVSPRFQRPNDVTRIIGYTVRNSLRVTVRDL
SNLGLIILDALVRAGSNLSRISFGISNEADLRDQARELAVKDAVRRATLLTAAAGTGLGK
VLSIREGGRSTGGFSAQVRARREAEVPIAPGELQVSARVTLEIELVG*
```

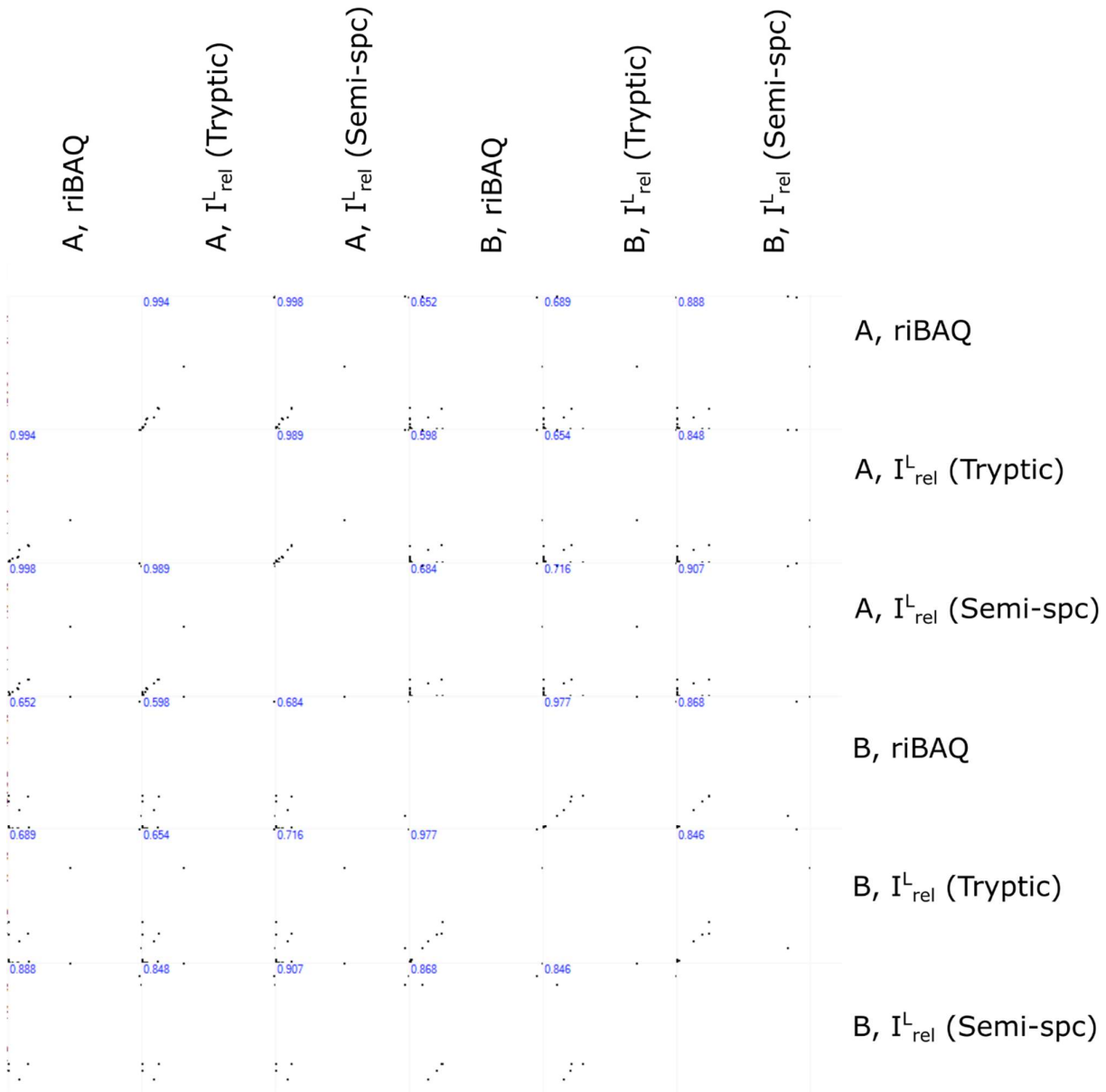
406

407 Figure 3: Protein sequence and experimental sequence coverage across both extracts and analysis methods  
408 (highlighted in grey) for the three most abundant *E. denticulatum* proteins identified. All three proteins  
409 passed final selection criteria (Stage 3) and accounted for 82.2% and 76.4% (quantified by  $I^L_{rel}$  using semi-  
410 specific analysis) of the verified, seaweed-specific proteins in extracts A and B, respectively. Including the  
411 isoform of c7052\_g1\_i1 (c7052\_g1\_i1 – not shown), the proteins account for 86.4% and 83.2%,  
412 respectively.

413

414 Filtering resulted in improved correlation between the two extracts up to a PCC of 0.91 for relative  
415 abundances quantified by  $I^L_{rel}$  (Figure 4). This indicates that in light of all the complications, the two protein  
416 extracts are in fact comparable, when all redundancy and contamination was addressed. Furthermore, the  
417 in-sample correlation between riBAQ and  $I^L_{rel}$  (PCC 0.87-1.0) indicated that  $I^L_{rel}$  may in fact be quite  
418 powerful analogue to riBAQ for non-standard (i.e. semi- or unspecific) analysis. As semi-specific in most  
419 cases increase both number of identified peptides as well as the sequence coverage on the individual  
420 protein level  $I^L_{rel}$  could be a powerful tool in the analysis of proteins where partial (non-specific) hydrolysis  
421 is observed, as this will include all peptide originating from the parent proteins rather than proteolytic  
422 peptides alone.

423



424

425 Figure 4: Correlation of relative protein abundances between extracts (A and B), analysis conditions (tryptic  
426 and semi-specific), and quantification method (riBAQ and  $I^L_{rel}$ ) following manual validation, filtering, and re-  
427 quantification (Stage 3). Pearson Correlation Coefficients are shown in blue in the upper left corner of each  
428 sub-plot.

429

430 Considering the level of contamination in the extracts as outlined above, this naturally affects the potential  
431 yield in targeted processing of the proteins. Including all initially identified peptides/protein including the  
432 common contaminants, the final list of quantified proteins constitute 78% of the total protein for extract A  
433 but merely 6.0% of the total protein for extract B. This correspond to the verified *E. denticulatum* proteins  
434 (Stage 3) constituting 5.6% and 4.2% of the total extract mass, based on the total protein content for the  
435 individual extracts. The observed level of contamination also indicated that although the total protein  
436 content was significantly increased in extract B, this may also come at a high cost in terms of applicability.  
437 However, as protein contamination can occur at all stages from processing facility to analysis lab, this  
438 should be investigated further. Furthermore, the tryptic analysis showed a significantly lower number of  
439 peptides and relative abundance for c6313\_g1\_i1.p1 compared to the semi-tryptic analysis for extract B.  
440 This could indicate that this particular protein is subject to partial hydrolysis during the additional  
441 processing, which again strengthens the use of the semi-specific analysis for this type of protein extract.  
442 The high degree of exogenous protein identified in extract B may also explain why the N-to-protein  
443 conversion factor of 5 appears to give much better results for extract A, and why extract B appears to be  
444 more accurately estimated using the Jones factor of 6.25 (Table 1).

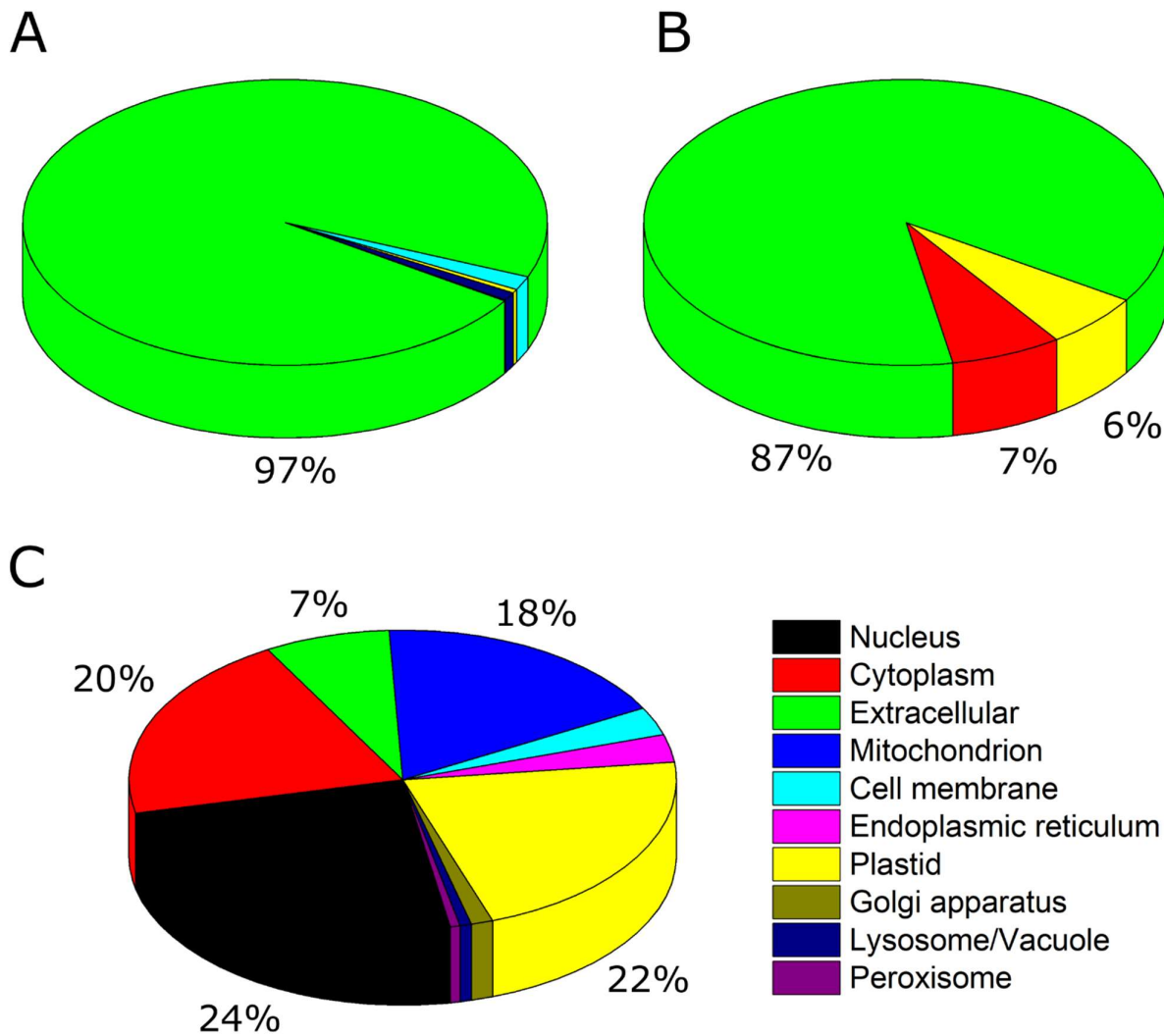
445

#### 446 *3.4. Enrichment of extracellular proteins*

447 In Figure 5, the relative subcellular distribution of proteins predicted by DeepLoc, is presented. For the  
448 transcriptome analysis (Fig 5C), a relative broad distribution of proteins (by rTPM) is observed with the  
449 majority of proteins being ascribed to the nucleus (24%), plastid (22%), cytoplasm (20%), mitochondria  
450 (18%), and extracellular (7%). This distribution does not correlate with the protein distribution established  
451 by LC-MS/MS, regardless of data analysis conditions employed. In fact, there is a very significant  
452 enrichment in extracellular proteins. For extract A (Fig 5A), almost exclusively extracellular proteins are  
453 identified (97%) by  $I^L_{rel.}$ . While extract B (Fig 5B) has some content of plastid and cytoplasmic protein, the

454 majority of identified proteins are extracellular (87%) by  $I^L_{rel}$ . The three primary proteins in both extracts  
455 are all classified as being extracellular. Although c7052\_g1\_i1.p1 shows homology to a periplasmic proteins  
456 by BlastP, it has a very high extracellular localization probability using DeepLoc (Table 2). At the individual  
457 protein level, the extracellular protein with the highest rTPM of 1.1%, c17304\_g1\_i1.p1 (see Table A.3), was  
458 determined to constitute 3.2-3.5% of the molar protein content. Although still significantly abundant, the  
459 three highly abundant extracellular proteins described above ( $I^L_{rel}$  17-33% each) merely constituted 0.02-  
460 0.29% on the transcript level, indicating that the extraction method is not selective for extracellular  
461 proteins per se, but rather a few selected extracellular proteins.

462



463

464 Figure 5: Relative subcellular protein distribution as predicted by DeepLoc (Almagro Armenteros et al.,  
465 2017) for A: Protein extract A. B: Protein extract B. For both protein extracts, relative abundance was  
466 estimated by  $I^L_{rel}$  through semi-tryptic analysis using optimized parameters, following manual inspection,  
467 validation, and filtering. C: Transcriptome analysis (by rTPM).

468

469 The fact that extracellular protein were almost exclusively identified in the extracts, is also very likely to  
470 explain the low extraction yields observed at the pilot plant (unpublished data from CP Kelco). From 20 kg

471 of seaweed, 155 g material was obtained using a 1000 L extraction tank (Extract A). The protein content (by  
472 Kjeldahl-N and converted using the Jones factor) of 7.1% correspond to merely 11 g of protein following  
473 extraction corresponding to a protein yield of 0.055%. Further processing to concentrate protein by acid  
474 precipitation (Extract B) yielded 6.7 g of product with 71% protein corresponding to 4.8 g of protein and  
475 consequently a loss of 57% protein mass and thus an even lower yield (0.024%). These findings indicate  
476 that the hot-water extraction used to obtain the extracts, is not capable, to a significant degree, to disrupt  
477 cells and release intracellular proteins. Low protein yields using simple aqueous extraction from *E.*  
478 *denticulatum* has previously been reported in literature (Bjarnadóttir et al., 2018; Fleurence, Le Coeur,  
479 Mabeau, Maurice, & Landrein, 1995). This, in turn, implies that there is still a significant potential for  
480 protein extraction from the seaweed and other approaches such as for instance pressurized and  
481 supercritical fluid extraction (Herrero, Sánchez-Camargo, Cifuentes, & Ibáñez, 2015), addition of cofactors  
482 (Harnedy & FitzGerald, 2013a; Maehre, Edvinsen, Eilertsen, & Ellevoll, 2016), microwave-assisted  
483 extraction (Magnusson et al., 2019), ultrasound-assisted extraction (Bleakley & Hayes, 2017), or any  
484 combination thereof (Cermeño, Kleekayai, Amigo-Benavent, Harnedy-Rothwell, & FitzGerald, 2020), may  
485 be more suitable. Enzyme assisted extraction (EAE) is an emerging technology for seaweed protein  
486 extraction, showing great potential (Hardouin et al., 2016; Naseri, Marinho, Holdt, Bartela, & Jacobsen,  
487 2020; Terme et al., 2020; Vásquez, Martínez, & Bernal, 2019). In a recent study, enzyme assisted extraction  
488 of *E. denticulatum* increased the protein yield up to 60% using Alcalase® or Viscozyme® (0.2% w/w) at pH 7  
489 and room temperature (Naseri, Jacobsen, et al., 2020). The increased protein extraction efficiency was  
490 furthermore obtained without compromising the downstream carrageenan production. However, this  
491 method is not at present implemented by the carrageenan industry.

492

493 **4. Conclusion:**

494 Using *de novo* transcriptome assembly, we were able to construct a novel reference proteome for  
495 *E. denticulatum*, which was used to characterize two pilot-scale, hot-water extracts. Although further  
496 processing (extract B) increased protein content significantly (compared to extract A), the aqueous  
497 solubility of both was quite low and both extracts displayed a high degree of smear and a lack of distinct  
498 protein bands by SDS-PAGE. A slightly alkaline pH and addition of a small amount of detergent fully  
499 solubilized the protein. From proteomics studies, using label-free quantification of non-standard protein  
500 digests via a novel length-normalized relative abundance approach, we determined that further extract  
501 processing may have introduced a significant amount of contaminant proteins not originating from the  
502 seaweed. After filtering of contaminant proteins and potential false-positive protein identifications, the  
503 protein content from the two extracts correlated quite well. Using subcellular localization prediction, we  
504 determined that both extracts were highly enriched in extracellular protein compared to the expected  
505 protein distribution from quantitative transcriptome analysis and estimated protein copy number. In fact,  
506 more than 75% of the seaweed-specific protein identified and quantified, was constituted by merely three  
507 proteins, which were predicted to be extracellular. Extracellular protein enrichment indicates that hot-  
508 water extraction is not capable of extracting intracellular proteins, but may be useful for isolation of  
509 extracellular protein content on large, industrial scale. Further processing of seaweed extracts is useful for  
510 increasing total protein content, but it requires further optimization to reduce the introduction of a large  
511 degree of exogenous protein, the depletion of species-specific proteins, and the significant loss in total  
512 protein. Nevertheless, this study illustrates the applicability of quantitative proteomics for characterization  
513 of extracts to be used as potential sources of novel food protein or bioactive peptides. Furthermore, the  
514 results clearly demonstrate the power of the methodology, particularly in combination with quantitative  
515 transcriptomics and bioinformatics, for evaluating extraction methods and for use as a guide in the  
516 development and optimization of industrial processes.

517

518 **5. Acknowledgements**

519 The authors would like to thank CP Kelco and in particular, Senior Scientist Jimmy Sejberg for supplying the  
520 seaweed protein extracts and for fruitful discussions related to analysis and manuscript preparation.

521

522 **6. Funding**

523 This work was supported by Innovation Fund Denmark (Grant number 7045-00021B (PROVIDE)).

524

525 **7. Author Contribution**

526 S.G.: Conceptualization, Methodology, Formal analysis, Investigation, Writing – original draft preparation,  
527 Writing – review and editing, Visualization. M.P.: Methodology, Formal analysis, Investigation, Writing –  
528 original draft preparation, Writing – review and editing. P.M.: Conceptualization, Methodology, Writing –  
529 review and editing, Supervision. S.L.H.: Writing – original draft preparation, Writing – review and editing.  
530 C.J.: Writing – original draft preparation, Writing – review and editing, Funding acquisition. P.J.G-M.:  
531 Methodology, Writing – review and editing. E.B.H.: Conceptualization, Writing – review and editing, Project  
532 administration, Funding acquisition. M.T.O.: Conceptualization, Writing – review and editing, Supervision.

533

534 **8. Conflict of Interest**

535 The authors declare no conflict of interest.

536

537 **9. Data Availability**

538 MaxQuant output files (txt folder) can be accessed through the linked Mendeley Data repository  
539 (Gregersen, 2020). Raw MS data can be made available upon request.

540

541 **References**

542 Admassu, H., Gasmalla, M. A. A., Yang, R., & Zhao, W. (2018). Bioactive Peptides Derived from Seaweed  
543 Protein and Their Health Benefits: Antihypertensive, Antioxidant, and Antidiabetic Properties. *Journal*  
544 *of Food Science*, 83(1), 6–16. <https://doi.org/10.1111/1750-3841.14011>

545 Almagro Armenteros, J. J., Sønderby, C. K., Sønderby, S. K., Nielsen, H., & Winther, O. (2017). DeepLoc:  
546 prediction of protein subcellular localization using deep learning. *Bioinformatics*, 33(21), 3387–3395.  
547 <https://doi.org/10.1093/bioinformatics/btx431>

548 Angell, A. R., Mata, L., de Nys, R., & Paul, N. A. (2016). The protein content of seaweeds: a universal  
549 nitrogen-to-protein conversion factor of five. *Journal of Applied Phycology*, 28(1), 511–524.  
550 <https://doi.org/10.1007/s10811-015-0650-1>

551 Bardou, P., Mariette, J., Escudié, F., Djemiel, C., & Klopp, C. (2014). Jvenn: An interactive Venn diagram  
552 viewer. *BMC Bioinformatics*, 15(1), 293. <https://doi.org/10.1186/1471-2105-15-293>

553 Bjarnadóttir, M., Aðalbjörnsson, B. V., Nilsson, A., Slizyte, R., Roleda, M. Y., Hreggviðsson, G. Ó., ...  
554 Jónsdóttir, R. (2018). Palmaria palmata as an alternative protein source: enzymatic protein extraction,  
555 amino acid composition, and nitrogen-to-protein conversion factor. *Journal of Applied Phycology*,  
556 30(3), 2061–2070. <https://doi.org/10.1007/s10811-017-1351-8>

557 Bleakley, S., & Hayes, M. (2017). Algal Proteins: Extraction, Application, and Challenges Concerning  
558 Production. *Foods*, 6(5), 33. <https://doi.org/10.3390/foods6050033>

559 Bolger, A. M., Lohse, M., & Usadel, B. (2014). Trimmomatic: A flexible trimmer for Illumina sequence data.  
560 *Bioinformatics*, 30(15), 2114–2120. <https://doi.org/10.1093/bioinformatics/btu170>

561 Cermeño, M., Kleekayai, T., Amigo-Benavent, M., Harnedy-Rothwell, P., & FitzGerald, R. J. (2020). Current  
562 knowledge on the extraction, purification, identification, and validation of bioactive peptides from

563 seaweed. *ELECTROPHORESIS*, elps.202000153. <https://doi.org/10.1002/elps.202000153>

564 Chart, H., & Rowe, B. (1991). Purification of lipopolysaccharide from strains of *Yersinia enterocolitica*  
565 belonging to serogroups 03 and 09. *FEMS Microbiology Letters*, 77(2–3), 341–346.  
566 <https://doi.org/10.1111/j.1574-6968.1991.tb04373.x>

567 Chen, C., Li, Z., Huang, H., Suzek, B. E., Wu, C. H., & Consortium, U. (2013). A Peptide Match service for  
568 UniProt Knowledgebase. *Bioinformatics*, 29(21), 2808–2809. Retrieved from  
569 <https://academic.oup.com/bioinformatics/article/29/21/2808/196283>

570 Cian, R. E., Garzón, A. G., Ancona, D. B., Guerrero, L. C., & Drago, S. R. (2015). Hydrolyzates from Pyropia  
571 columbina seaweed have antiplatelet aggregation, antioxidant and ACE I inhibitory peptides which  
572 maintain bioactivity after simulated gastrointestinal digestion. *LWT - Food Science and Technology*,  
573 64(2), 881–888. <https://doi.org/10.1016/j.lwt.2015.06.043>

574 Cox, J., & Mann, M. (2008). MaxQuant enables high peptide identification rates, individualized p.p.b.-range  
575 mass accuracies and proteome-wide protein quantification. *Nature Biotechnology*, 26(12), 1367–  
576 1372. <https://doi.org/10.1038/nbt.1511>

577 Cox, J., Neuhauser, N., Michalski, A., Scheltema, R. A., Olsen, J. V., & Mann, M. (2011). Andromeda: A  
578 peptide search engine integrated into the MaxQuant environment. *Journal of Proteome Research*,  
579 10(4), 1794–1805. <https://doi.org/10.1021/pr101065j>

580 El-Gebali, S., Mistry, J., Bateman, A., Eddy, S. R., Luciani, A., Potter, S. C., ... Finn, R. D. (2018). The Pfam  
581 protein families database in 2019. *Nucleic Acids Research*, 47, 427–432.  
582 <https://doi.org/10.1093/nar/gky995>

583 Elliott, S., Egrie, J., Browne, J., Lorenzini, T., Busse, L., Rogers, N., & Ponting, I. (2004). Control of rHuEPO  
584 biological activity: The role of carbohydrate. *Experimental Hematology*, 32(12), 1146–1155.  
585 <https://doi.org/10.1016/j.exphem.2004.08.004>

586 Fernandez-Patron, C., Calero, M., Collazo, P. R., Garcia, J. R., Madrazo, J., Musacchio, A., ... Mendez, E.

587 (1995). Protein Reverse Staining: High-Efficiency Microanalysis of Unmodified Proteins Detected on

588 Electrophoresis Gels. *Analytical Biochemistry*, 224(1), 203–211.

589 <https://doi.org/10.1006/ABIO.1995.1031>

590 Finn, R. D., Clements, J., & Eddy, S. R. (2011). HMMER web server: interactive sequence similarity searching.

591 *Nucleic Acids Research*, 39, W29–W37. <https://doi.org/10.1093/nar/gkr367>

592 Finn, R. D., Mistry, J., Tate, J., Coggill, P., Heger, A., Pollington, J. E., ... Bateman, A. (2010). The Pfam protein

593 families database. *Nucleic Acids Research*, 38, D211–D222. <https://doi.org/10.1093/nar/gkp985>

594 Fitzgerald, C., Mora-Soler, L., Gallagher, E., O'Connor, P., Prieto, J., Soler-Vila, A., & Hayes, M. (2012).

595 Isolation and characterization of bioactive pro-peptides with in Vitro renin inhibitory activities from

596 the macroalga *Palmaria palmata*. *Journal of Agricultural and Food Chemistry*, 60(30), 7421–7427.

597 <https://doi.org/10.1021/jf301361c>

598 Fleurence, J., Le Coeur, C., Mabeau, S., Maurice, M., & Landrein, A. (1995). Comparison of different

599 extractive procedures for proteins from the edible seaweeds *Ulva rigida* and *Ulva rotundata*. *Journal*

600 *of Applied Phycology*, 7(6), 577–582. <https://doi.org/10.1007/BF00003945>

601 Furuta, T., Miyabe, Y., Yasui, H., Kinoshita, Y., & Kishimura, H. (2016). Angiotensin I Converting Enzyme

602 Inhibitory Peptides Derived from Phycobiliproteins of Dulse *Palmaria palmata*. *Marine Drugs*, 14(2),

603 32. <https://doi.org/10.3390/md14020032>

604 García-Moreno, P. J., Gregersen, S., Nedamani, E. R., Olsen, T. H., Marcatili, P., Overgaard, M. T., ...

605 Jacobsen, C. (2020). Identification of emulsifier potato peptides by bioinformatics: application to

606 omega-3 delivery emulsions and release from potato industry side streams. *Scientific Reports*, 10(1),

607 690. <https://doi.org/10.1038/s41598-019-57229-6>

608 García-Moreno, P. J., Jacobsen, C., Marcatili, P., Gregersen, S., Overgaard, M. T., Andersen, M. L., ... Hansen,

609 E. B. (2020). Emulsifying peptides from potato protein predicted by bioinformatics: Stabilization of fish  
610 oil-in-water emulsions. *Food Hydrocolloids*, 101. <https://doi.org/10.1016/j.foodhyd.2019.105529>

611 Gomez-Zavaglia, A., Prieto Lage, M. A., Jimenez-Lopez, C., Mejuto, J. C., & Simal-Gandara, J. (2019,  
612 September 1). The potential of seaweeds as a source of functional ingredients of prebiotic and  
613 antioxidant value. *Antioxidants*, Vol. 8, p. 406. <https://doi.org/10.3390/antiox8090406>

614 Grabherr, M. G., Haas, B. J., Yassour, M., Levin, J. Z., Thompson, D. A., Amit, I., ... Regev, A. (2011). Full-  
615 length transcriptome assembly from RNA-Seq data without a reference genome. *Nature  
616 Biotechnology*, 29(7), 644–652. <https://doi.org/10.1038/nbt.1883>

617 Gregersen, S. (2020). E.denticulatum quant BUP. *Mendeley Data*, V1.  
618 <https://doi.org/10.17632/y4kmnb3tvx.1>

619 Hardouin, K., Bedoux, G., Burlot, A. S., Donnay-Moreno, C., Bergé, J. P., Nyvall-Collén, P., & Bourgougnon,  
620 N. (2016). Enzyme-assisted extraction (EAE) for the production of antiviral and antioxidant extracts  
621 from the green seaweed *Ulva armoricana* (Ulvales, Ulvophyceae). *Algal Research*, 16, 233–239.  
622 <https://doi.org/10.1016/j.algal.2016.03.013>

623 Harnedy, P. A., & FitzGerald, R. J. (2013a). Extraction of protein from the macroalga *Palmaria palmata*. *LWT  
624 - Food Science and Technology*, 51(1), 375–382. <https://doi.org/10.1016/j.lwt.2012.09.023>

625 Harnedy, P. A., & FitzGerald, R. J. (2013b). In vitro assessment of the cardioprotective, anti-diabetic and  
626 antioxidant potential of *Palmaria palmata* protein hydrolysates. *Journal of Applied Phycology*, 25(6),  
627 1793–1803. <https://doi.org/10.1007/s10811-013-0017-4>

628 Hashimoto, A., & Pickard, M. A. (1984). Chloroperoxidases from *Caldariomyces* (= *Leptoxiphium*) Cultures:  
629 Glycoproteins with Variable Carbohydrate Content and Isoenzymic Forms. *Microbiology*, 130(8),  
630 2051–2058. <https://doi.org/10.1099/00221287-130-8-2051>

631 Herrero, M., Sánchez-Camargo, A. del P., Cifuentes, A., & Ibáñez, E. (2015, September 1). Plants, seaweeds,

632 microalgae and food by-products as natural sources of functional ingredients obtained using  
633 pressurized liquid extraction and supercritical fluid extraction. *TrAC - Trends in Analytical Chemistry*,  
634 Vol. 71, pp. 26–38. <https://doi.org/10.1016/j.trac.2015.01.018>

635 Holdt, S. L., & Kraan, S. (2011, June 9). Bioactive compounds in seaweed: Functional food applications and  
636 legislation. *Journal of Applied Phycology*, Vol. 23, pp. 543–597. <https://doi.org/10.1007/s10811-010-9632-5>

638 Jafarpour, A., Gomes, R. M., Gregersen, S., Sloth, J. J., Jacobsen, C., & Moltke Sørensen, A. D. (2020).  
639 Characterization of cod (*Gadus morhua*) frame composition and its valorization by enzymatic  
640 hydrolysis. *Journal of Food Composition and Analysis*, 89, 103469.  
641 <https://doi.org/10.1016/j.jfca.2020.103469>

642 Jafarpour, A., Gregersen, S., Gomes, R. M., Marcatili, P., Olsen, T. H., Jacobsen, C., ... Sørensen, A.-D. M.  
643 (2020). Biofunctionality of enzymatically derived peptides from codfish (*Gadus morhua*) frame: Bulk in  
644 vitro properties, quantitative proteomics, and bioinformatic prediction. *Preprints*.  
645 <https://doi.org/10.20944/preprints202011.0195.v1>

646 Jones, D. B. (1931). Factors for Converting Percentages of Nitrogen in Foods and Feeds Into percentages of  
647 protein. Retrieved July 20, 2020, from US Department of Agriculture website:  
648 [https://books.google.dk/books?hl=en&lr=&id=MaM4Z51DcjoC&oi=fnd&pg=PA9&ots=QAQAI-eXWv&sig=edeezmYHONz\\_m89QRHtgI-94oGg&redir\\_esc=y#v=onepage&q&f=false](https://books.google.dk/books?hl=en&lr=&id=MaM4Z51DcjoC&oi=fnd&pg=PA9&ots=QAQAI-eXWv&sig=edeezmYHONz_m89QRHtgI-94oGg&redir_esc=y#v=onepage&q&f=false)

650 Leandro, A., Pacheco, D., Cotas, J., Marques, J. C., Pereira, L., & Gonçalves, A. M. M. (2020, August 1).  
651 Seaweed's bioactive candidate compounds to food industry and global food security. *Life*, Vol. 10, pp.  
652 1–37. <https://doi.org/10.3390/life10080140>

653 Liu, F., Baggerman, G., Schoofs, L., & Wets, G. (2008). The construction of a bioactive peptide database in  
654 metazoa. *Journal of Proteome Research*, 7(9), 4119–4131. <https://doi.org/10.1021/pr800037n>

655 Madden, T. (2013). The BLAST Sequence Analysis Tool. In *The NCBI Handbook [Internet]. 2nd edition.*

656 Retrieved from <https://www.ncbi.nlm.nih.gov/books/NBK153387/>

657 Maehre, H. K., Edvinsen, G. K., Eilertsen, K. E., & Ellevoll, E. O. (2016). Heat treatment increases the protein

658 bioaccessibility in the red seaweed dulse (*Palmaria palmata*), but not in the brown seaweed winged

659 kelp (*Alaria esculenta*). *Journal of Applied Phycology*, 28(1), 581–590. <https://doi.org/10.1007/s10811-015-0587-4>

661 Magnusson, M., Glasson, C. R. K., Vucko, M. J., Angell, A., Neoh, T. L., & de Nys, R. (2019). Enrichment

662 processes for the production of high-protein feed from the green seaweed *Ulva ohnoi*. *Algal Research*,

663 41, 101555. <https://doi.org/10.1016/j.algal.2019.101555>

664 Mariotti, F., Tomé, D., & Mirand, P. P. (2008). Converting nitrogen into protein - Beyond 6.25 and Jones'

665 factors. *Critical Reviews in Food Science and Nutrition*, 48(2), 177–184.

666 <https://doi.org/10.1080/10408390701279749>

667 Minkiewicz, P., Iwaniak, A., & Darewicz, M. (2019). BIOPEP-UWM Database of Bioactive Peptides: Current

668 Opportunities. *International Journal of Molecular Sciences*, 20(23).

669 <https://doi.org/10.3390/ijms20235978>

670 Møller, H. J., & Poulsen, J. H. (2009). Staining of Glycoproteins/Proteoglycans on SDS-Gels. In J. M. Walker

671 (Ed.), *The Protein Protocols Handbook. Springer Protocols Handbooks* (pp. 569–574).

672 [https://doi.org/10.1007/978-1-59745-198-7\\_52](https://doi.org/10.1007/978-1-59745-198-7_52)

673 Mooney, C., Haslam, N. J., Holton, T. A., Pollastri, G., & Shields, D. C. (2013). PeptideLocator: prediction of

674 bioactive peptides in protein sequences. *Bioinformatics (Oxford, England)*, 29(9), 1120–1126.

675 <https://doi.org/10.1093/bioinformatics/btt103>

676 Mooney, C., Haslam, N. J., Pollastri, G., & Shields, D. C. (2012). Towards the Improved Discovery and Design

677 of Functional Peptides: Common Features of Diverse Classes Permit Generalized Prediction of

678 Bioactivity. *PLoS ONE*, 7(10), e45012. <https://doi.org/10.1371/journal.pone.0045012>

679 Naseri, A., Jacobsen, C., Sejberg, J. J. P., Pedersen, T. E., Larsen, J., Hansen, K. M., & Holdt, S. L. (2020).

680 Multi-Extraction and Quality of Protein and Carrageenan from Commercial Spinosum (Eucheuma  
681 denticulatum). *Foods*, 9(8), 1072. <https://doi.org/10.3390/foods9081072>

682 Naseri, A., Marinho, G. S., Holdt, S. L., Bartela, J. M., & Jacobsen, C. (2020). Enzyme-assisted extraction and  
683 characterization of protein from red seaweed *Palmaria palmata*. *Algal Research*, 47, 101849.  
684 <https://doi.org/10.1016/j.algal.2020.101849>

685 Olsen, T. H., Yesiltas, B., Marin, F. I., Pertseva, M., García-Moreno, P. J., Gregersen, S., ... Marcatili, P. (2020).

686 AnOxPePred: using deep learning for the prediction of antioxidative properties of peptides. *Scientific  
687 Reports*, 10(1), 21471. <https://doi.org/10.1038/s41598-020-78319-w>

688 Panyayai, T., Ngamphiw, C., Tongsima, S., Mhuantong, W., Limsripraphan, W., Choowongkomon, K., &  
689 Sawatdichaikul, O. (2019). PeptideDB: A web application for new bioactive peptides from food  
690 protein. *Helicon*, 5(7). <https://doi.org/10.1016/j.heliyon.2019.e02076>

691 Park, J., Kim, K. J., Choi, K. S., Grab, D. J., & Dumler, J. S. (2004). *Anaplasma phagocytophilum* AnkA binds to  
692 granulocyte DNA and nuclear proteins. *Cellular Microbiology*, 6(8), 743–751.  
693 <https://doi.org/10.1111/j.1462-5822.2004.00400.x>

694 Peñalver, R., Lorenzo, J. M., Ros, G., Amarowicz, R., Pateiro, M., & Nieto, G. (2020). Seaweeds as a  
695 Functional Ingredient for a Healthy Diet. *Marine Drugs*, 18(6), 301.  
696 <https://doi.org/10.3390/MD18060301>

697 Porse, H. (2018). The Seaweed Processing Industry. *Seaweed Network of Denmark, 10th Anniversary*.  
698 Copenhagen.

699 Rappaport, J., Mann, M., & Ishihama, Y. (2007). Protocol for micro-purification, enrichment, pre-  
700 fractionation and storage of peptides for proteomics using StageTips. *Nature Protocols*, 2(8), 1896–

701 1906. <https://doi.org/10.1038/nprot.2007.261>

702 Rosni, M., Fisal, A., Azwan, A., Chye, F. Y., Matanjun, P., Mohd Rosni, S., ... Matanjun, P. (2015). Crude  
703 proteins, total soluble proteins, total phenolic contents and SDS-PAGE profile of fifteen varieties of  
704 seaweed from Semporna, Sabah, Malaysia. *International Food Research Journal*, 22(4), 1483–1493.

705 Retrieved from  
706 <https://search.proquest.com/docview/1698633507/fulltextPDF/CBDD91AFF68E4050PQ/1?accountid=8144>

708 Salo-Väänänen, P. P., & Koivistoinen, P. E. (1996). Determination of protein in foods: Comparison of net  
709 protein and crude protein (N x 6.25) values. *Food Chemistry*, 57(1), 27–31.  
710 [https://doi.org/10.1016/0308-8146\(96\)00157-4](https://doi.org/10.1016/0308-8146(96)00157-4)

711 Schwanhäusser, B., Busse, D., Li, N., Dittmar, G., Schuchhardt, J., Wolf, J., ... Selbach, M. (2011). Global  
712 quantification of mammalian gene expression control. *Nature*, 473(7347), 337–342.  
713 <https://doi.org/10.1038/nature10098>

714 Shevchenko, A., Wilm, M., Vorm, O., & Mann, M. (1982). Techniques in Protein Chemistry V. In *Mass  
715 Spectrometry in the Biological Sciences* (Vol. 258). Retrieved from Humana Press website:  
716 <https://pubs.acs.org/sharingguidelines>

717 Shin, J. B., Krey, J. F., Hassan, A., Metlagel, Z., Tauscher, A. N., Pagana, J. M., ... Barr-Gillespie, P. G. (2013).  
718 Molecular architecture of the chick vestibular hair bundle. *Nature Neuroscience*, 16(3), 365–374.  
719 <https://doi.org/10.1038/nn.3312>

720 Simões-Barbosa, A., Santana, J. M., & Teixeira, A. R. L. (2000). Solubilization of delipidated macrophage  
721 membrane proteins for analysis by two-dimensional electrophoresis. *ELECTROPHORESIS*, 21(3), 641–  
722 644. [https://doi.org/10.1002/\(SICI\)1522-2683\(20000201\)21:3<641::AID-ELPS641>3.0.CO;2-H](https://doi.org/10.1002/(SICI)1522-2683(20000201)21:3<641::AID-ELPS641>3.0.CO;2-H)

723 Sparbier, K., Koch, S., Kessler, I., Wenzel, T., & Kostrzewska, M. (2005). Selective isolation of glycoproteins and

724 glycopeptides for MALDI-TOF MS detection supported by magnetic particles. *Journal of Biomolecular*  
725 *Techniques*, 16(4), 407–411.

726 Terme, N., Hardouin, K., Cortès, H. P., Peñuela, A., Freile-Pelegrín, Y., Robledo, D., ... Bourgougnon, N.  
727 (2020). Emerging seaweed extraction techniques: Enzyme-assisted extraction a key step of seaweed  
728 biorefinery? In *Sustainable Seaweed Technologies* (pp. 225–256). <https://doi.org/10.1016/b978-0-12->  
729 817943-7.00009-3

730 Tiwary, S., Levy, R., Gutenbrunner, P., Salinas Soto, F., Palaniappan, K. K., Deming, L., ... Cox, J. (2019). High-  
731 quality MS/MS spectrum prediction for data-dependent and data-independent acquisition data  
732 analysis. *Nature Methods*, 16(6), 519–525. <https://doi.org/10.1038/s41592-019-0427-6>

733 Tu, M., Cheng, S., Lu, W., & Du, M. (2018, August 1). Advancement and prospects of bioinformatics analysis  
734 for studying bioactive peptides from food-derived protein: Sequence, structure, and functions. *TrAC -*  
735 *Trends in Analytical Chemistry*, Vol. 105, pp. 7–17. <https://doi.org/10.1016/j.trac.2018.04.005>

736 Tyanova, S., & Cox, J. (2018). *Perseus: A Bioinformatics Platform for Integrative Analysis of Proteomics Data*  
737 *in Cancer Research*. [https://doi.org/10.1007/978-1-4939-7493-1\\_7](https://doi.org/10.1007/978-1-4939-7493-1_7)

738 Tyanova, S., Temu, T., & Cox, J. (2016). The MaxQuant computational platform for mass spectrometry-  
739 based shotgun proteomics. *Nature Protocols*, 11(12), 2301–2319.  
740 <https://doi.org/10.1038/nprot.2016.136>

741 Tyanova, S., Temu, T., Sinitcyn, P., Carlson, A., Hein, M. Y., Geiger, T., ... Cox, J. (2016, August 30). The  
742 Perseus computational platform for comprehensive analysis of (prote)omics data. *Nature Methods*,  
743 Vol. 13, pp. 731–740. <https://doi.org/10.1038/nmeth.3901>

744 Vásquez, V., Martínez, R., & Bernal, C. (2019). Enzyme-assisted extraction of proteins from the seaweeds  
745 *Macrocystis pyrifera* and *Chondracanthus chamussoi*: characterization of the extracts and their  
746 bioactive potential. *Journal of Applied Phycology*, 31(3), 1999–2010. <https://doi.org/10.1007/s10811->

747 018-1712-y

748 Wang, G., Li, X., & Wang, Z. (2009). APD2: the updated antimicrobial peptide database and its application in

749 peptide design. *Nucleic Acids Research*, 37, D933–D937. Retrieved from

750 [https://academic.oup.com/nar/article/37/suppl\\_1/D933/1013124](https://academic.oup.com/nar/article/37/suppl_1/D933/1013124)

751 Wang, W., Vignani, R., Scali, M., Sensi, E., Tiberi, P., & Cresti, M. (2004). Removal of lipid contaminants by

752 organic solvents from oilseed protein extract prior to electrophoresis. *Analytical Biochemistry*, 329,

753 139–141. <https://doi.org/10.1016/j.ab.2004.02.044>

754